GEOPHYSICAL RESEARCH LETTERS, VOL. 34, L02302, doi:10.1029/2006GL027586, 2007

Kinematics of the Nicaraguan forearc from GPS geodesy

Henry L. Turner III,[1,2] Peter LaFemina,[3] Armando Saballos,[4] Glen S. Mattioli,[2] Pamela E. Jansma,[1,2] and Timothy Dixon[5]

Received 21 July 2006; revised 21 November 2006; accepted 6 December 2006; published 24 January 2007.

[1] Campaign GPS data from a network in the Nicaraguan forearc show a strong component of arc-parallel motion indicating northwest translation of a nearly rigid forearc sliver. Our measured mean velocity for forearc sites of 15.1 mm yr^{-1} agrees well with the arc-parallel sliver motion predicted previously by DeMets (2001) derived from closure constraints on oblique convergence between the Cocos and Caribbean plates. The lack of a northeasterly oriented arc-normal component of motion in forearc velocities indicates that there are complexities involved beyond a simple interpretation of sliver motion being driven by oblique convergence. The forearc is reasonably well-fit by rigid rotation about an Euler pole with a rms misfit of residual velocities of 4.9 ± 2.6 mm yr^{-1}. Current motion of the forearc sliver relative to the stable Caribbean plate yields predominantly boundary parallel NW motion with boundary normal extension in the northwestern region averaging ~5 mm yr^{-1}. **Citation:** Turner, H. L., III, P. LaFemina, A. Saballos, G. S. Mattioli, P. E. Jansma, and T. Dixon (2007), Kinematics of the Nicaraguan forearc from GPS geodesy, *Geophys. Res. Lett.*, *34*, L02302, doi:10.1029/2006GL027586.

1. Introduction

[2] Northwestward translation of a forearc sliver in Nicaragua resulting from oblique convergence between the Cocos (CO) and Caribbean (CA) plates has been suggested by several previous studies [e.g., *Harlow and White*, 1985; *White*, 1991]. Arc-parallel motion of the forearc averaging ~7–8 mm yr^{-1}on the Nicoya Peninsula of Costa Rica has been observed geodetically by *Lundgren et al.* [1999] and *Norabuena et al.* [2004] and modeled as a rigid block rotation by *McCaffrey* [2002]. *DeMets* [2001] made the first attempt to quantify the slip rate of forearc sliver motion in Nicaragua through comparison of a newly calculated CO-CA convergence vector with the compressional axes of earthquake focal mechanisms for shallow thrust events believed to have occurred along the plate interface. This study predicted a slip rate of 14 ± 2 mm yr^{-1} for the forearc sliver in Nicaragua. No geodetic measurements from the forearc were included in *DeMets' [2001]* calculations, but he noted that early results from the continuous GPS site MANA, in Managua, gave a velocity of 10 ± 4 mm yr^{-1} to the Northwest. Here we report the geodetic velocity field for a network of campaign GPS sites in the Nicaraguan forearc and backarc, and compare the observed velocity field with the predicted forearc sliver velocity of *DeMets* [2001]. We also test whether the forearc may be modeled as a distinct block independent of the rigid Caribbean plate [*Jansma et al.*, 2000; *Jansma and Mattioli*, 2005].

2. GPS Data Acquisition and Processing

[3] Initial campaign GPS measurements in the Nicaraguan forearc were made on a network of 10 sites in August 2000. Six additional sites were installed in early 2001. The network was occupied again in August 2002 and in February 2003. Additional data collected in early 2006 record the coseismic and postseismic effects of the M_w6.9 Oct. 9, 2004 earthquake off the coast of Nicaragua and are not used for this interseismic analysis.

[4] Campaign measurements were made using Trimble 4000SSi and Ashtech Z-12 dual frequency GPS receivers that record both L1 and L2 code and phase data (Figure 1 and Table 1). All receivers were used with Dorn-Margolin choke-ring antennae. Observations on each site were made for a minimum of three consecutive UTC days with a 30 second sampling interval and an elevation mask of 10°.

[5] Data were also acquired from two continuous GPS sites in Nicaragua (MANA and ESTI), one continuous site in El Salvador (SSIA), and three sites in Honduras (TEGU, TEG1, and SLOR). TEG1 replaced TEGU and we have tied the time-series for the two together and hereafter refer to the combined time-series as TEG1. All available data for these sites were downloaded from SOPAC.

[6] All GPS data were processed with an absolute point positioning strategy using GIPSY-OASIS II (version 2.5.8a), and precise clock and orbit parameters provided by JPL (see *Jansma et al.* [2000] and *Jansma and Mattioli* [2005] for additional details on our processing procedures). The error analysis strategy of *Mao et al.* [1999] using a model for time-correlated and white noise was used to evaluate error in velocity time series and the final errors include a fixed value of 2 mm/sqrt (yr) of monument noise. Station positions and their covariances were then converted from the International Terrestrial Reference Frame 2000 (ITRF00), into an updated version of the GPS-derived Caribbean plate reference frame of *DeMets et al.* [2007]. Finally, we applied a common-mode noise filter to the time series as described by *Marquez-Azua and DeMets* [2003]. In our analysis, most sites had at least 3 epochs of observations, although CHIN, CORI, PUEC, TRAN, and VINC site motions were con-

[1]Arkansas Center for Space and Planetary Sciences, University of Arkansas, Fayetteville, Arkansas, USA.
[2]Department of Geosciences, University of Arkansas, Fayetteville, Arkansas, USA.
[3]Department of Geosciences, Pennsylvania State University, University Park, Pennsylvania, USA.
[4]Instituto Nicaragüense de Estudios Territoriales, Managua, Nicaragua.
[5]Rosenstiel School of Marine and Atmospheric Science, University of Miami, Miami, Florida, USA.

0094-8276/07/2006GL027586$05.00

Table 1. Campaign and Continuous GPS Site Locations and Velocities in Nicaraguan Network Determined for this Study

Site	Lat., °N	Long., °E	HAE[a], m	Time-Span years	Velocity wrt ITRF00[b] N mm/yr	Velocity wrt ITRF00[b] E mm/yr	Coseismic Offsets[c] N mm	Coseismic Offsets[c] E mm	Velocity wrt Caribbean[d] N mm/yr	Velocity wrt Caribbean[d] E mm/yr
Forearc										
ANA1	12.08	273.62	513.76	2.52	15.7 ± 3.2	−0.2 ± 5.0	0.44	1.69	10.7 ± 3.2	12.6 ± 5.0
CHIN	12.64	272.86	68.85	2.11	9.7 ± 4.0	−5.9 ± 5.6	-	-	5.2 ± 4.0	−17.4 ± 5.6
CORI	12.52	272.80	6.86	1.99	7.1 ± 3.3	−11.5 ± 4.7	-	-	2.6 ± 3.3	23.1 ± 4.7
ELBQ	11.28	274.33	48.06	3.84	13.0 ± 2.4	3.7 ± 3.4	0.20	0.62	7.8 ± 2.4	−8.6 ± 3.4
ELCO	12.81	272.60	24.98	2.53	8.7 ± 3.1	5.1 ± 4.9	2.18	6.19	3.4 ± 3.1	−8.7 ± 4.9
LEON	12.43	273.09	76.33	2.56	8.8 ± 3.0	−0.2 ± 4.6	0.87	2.99	3.8 ± 3.0	−13.0 ± 4.6
OCHO	11.66	274.04	59.71	2.51	17.1 ± 3.5	4.2 ± 6.9	0.28	0.97	12.1 ± 3.5	−8.1 ± 6.9
PAZC	12.30	273.41	55.89	2.53	14.6 ± 3.1	−6.1 ± 4.8	0.60	2.32	9.6 ± 3.1	−18.7 ± 4.8
POCH	11.77	273.49	13.26	2.55	11.2 ± 3.3	1.6 ± 5.3	0.44	1.04	6.2 ± 3.3	−10.7 ± 5.3
PONE	12.38	272.98	47.30	2.10	8.5 ± 3.6	−0.8 ± 5.6	0.94	2.80	3.5 ± 3.6	−13.7 ± 5.6
TRAN	12.03	273.31	28.54	2.07	14.2 ± 4.2	−2.7 ± 6.8	-	-	9.5 ± 4.2	−14.4 ± 6.8
VINC	11.29	274.10	14.80	2.06	13.1 ± 4.6	−7.7 ± 8.3	-	-	8.1 ± 4.6	−4.4 ± 8.3
Arc/Backarc										
MALP	12.55	273.32	214.39	3.49	8.9 ± 2.6	6.1 ± 5.5	0.82	3.25	4.0 ± 2.6	−6.4 ± 5.5
PORT	12.57	274.63	455.27	2.54	4.6 ± 3.3	10.6 ± 5.2	0.42	1.80	−0.8 ± 3.3	−1.6 ± 5.2
PUEC	14.04	276.62	23.25	2.10	5.8 ± 3.9	5.5 ± 6.2	-	-	−0.1 ± 3.9	−5.4 ± 6.2
RIOB	12.92	274.78	239.14	2.55	6.8 ± 3.2	8.6 ± 7.4	0.53	1.97	1.3 ± 3.2	−3.5 ± 7.4
TEUS	12.41	274.19	153.95	2.55	6.2 ± 3.3	9.8 ± 4.4	0.44	1.98	1.0 ± 3.3	−2.6 ± 4.4
Continuous										
ESTI	13.10	273.64	852.67	2.80	12.8 ± 1.4	8.6 ± 2.0	2.02	5.79	8.0 ± 1.4	−2.7 ± 2.0
MANA	12.15	273.75	71.05	4.38	10.1 ± 1.1	5.2 ± 1.4	0.32	1.08	5.3 ± 1.1	−6.5 ± 1.4
SLOR	13.42	272.56	12.00	1.85	2.8 ± 1.6	8.2 ± 2.6	6.02	8.36	−1.5 ± 1.6	−2.9 ± 2.6
SSIA	13.70	270.88	626.60	5.49	8.7 ± 1.2	4.6 ± 1.5	−12.22	6.89	5.0 ± 1.2	−6.4 ± 1.5
TEG1	14.09	272.79	951.340	3.940	6.8 ± 1.2	6.0 ± 1.4	5.98	9.23	2.3 ± 1.2	−4.8 ± 1.4

[a]HAE = Height above ellipsoid in meters. Geodetic coordinates are relative to WGS-84 reference ellipsoid.
[b]All errors reported are 1σ.
[c]Coseismic offsets predicted for campaign sites from elastic half-space dislocation model. Offsets given for continuous sites are values calculated from time-series. Campaign sites without offsets were not installed until after the Jan. 13, 2001 event.
[d]Velocity with respect to Caribbean following removal of coseismic offsets. Predicted Caribbean velocities are assumed to be perfectly known—thus errors associated with the Caribbean reference frame are not addressed.

strained by only two epochs (see auxiliary material[1] for time-series).

3. Continuous Network Results

[7] Velocities for the continuous GPS sites are given in Table 1 and shown in Figure 1. Time-series for SLOR and TEG1 in Honduras show offsets associated with coseismic displacement from the January 13, 2001 subduction zone earthquake off the coast of El Salvador. A gap in the available data for each site from around March 15, 2001 to May 10, 2001 obscures part of the post-seismic record, but there appears to be no significant coseismic offset related to the February 13, 2001 earthquake near San Salvador. The calculated coseismic offsets were removed from time-series for SLOR and TEG1 to derive interseismic linear velocities for these two sites. SLOR has a small residual velocity of 3.3 ± 3.1 mm yr^{-1} to the southwest, while TEG1 gives a velocity of 5.3 ± 1.8 mm yr^{-1} to the northwest. The SLOR time-series has the shortest duration (<2 yrs) and as such the interseismic velocity for this site should be considered preliminary. The time-series for SSIA shows coseismic offsets associated with both the January 13, 2001 earthquake and the February 13, 2001 earthquake near San Salvador. The calculated coseismic offsets were removed from the SSIA time series to derive the interseismic linear velocity of 8.1 ± 1.9 mm yr^{-1} to the northwest. Although, there is no readily identifiable coseismic displacement apparent in the ESTI and MAN A time-series, we have calculated offsets using the time-series for this event, which agree well with our model predictions. The time series for MANA gives a velocity with a similar direction as those from forearc campaign sites, but with a lower magnitude (8.4 ± 1.8 mm yr^{-1}). The time-series for ESTI gives a north-northwest directed velocity with a magnitude of 8.4 ± 2.4 mm yr^{-1}. We suspect that the ESTI site may be biased by a signal related to monument instability because the antenna is mounted at the top of a ~15 m weak steel tower secured by guy wires which have been adjusted during the period of observation.

4. The January 13, 2001 El Salvador Earthquake

[8] Interpretation of our campaign time-series is complicated by the possible coseismic and post-seismic effects of the M_w 7.7 earthquake which occurred off the coast of El Salvador on January 13, 2001. As discussed above, significant coseismic offsets were observed in continuous GPS sites in El Salvador and Honduras. Similar offsets are expected to have occurred at our northern campaign sites, but cannot be directly constrained due to the lack of sufficient data immediately before and after the earthquake. To address this, we developed an elastic half-space dislocation model using the parameters for fault rupture given by *Bommer et al.* [2002]. We found that the observed offsets in the continuous sites SSIA, SLOR, and TEG1 were well-fit by 80 cm of normal slip on a 65 km long, 55 km wide

[1]Auxiliary materials are available in the HTML. doi:10.1029/2006GL027586.

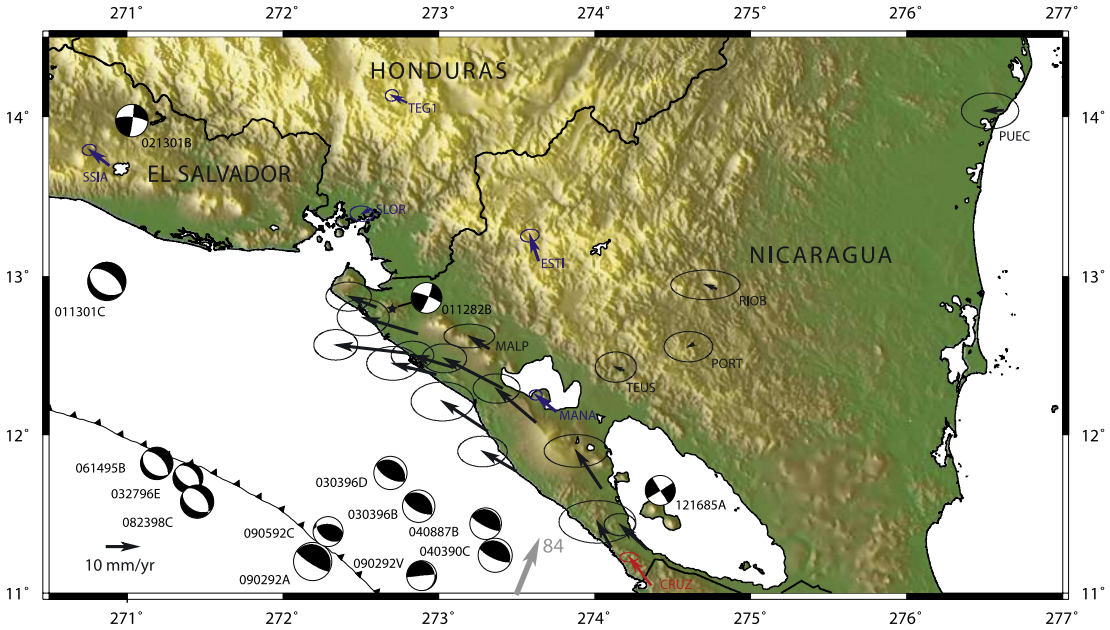

Figure 1. GPS velocity map of Nicaragua and surrounding region. Black arrows are campaign velocities for our network in Nicaragua. Names of forearc campaign sites are shown in Figure 2. Blue arrows are our calculated velocities of continuous sites in the region. Velocities are relative to the Caribbean plate reference frame of *DeMets et al.* [2007]. The red arrow is a velocity from *Norabuena et al.* [2004] in the Caribbean reference frame of *Sella et al.* [2002] for a Costa Rican site. The grey arrow is the 84 mm yr^{-1} CO-CA convergence direction of *DeMets* [2001] and is not to scale. Focal mechanisms are for events 1976–2003 with scalar moments of 10^{25} dyne cm or larger from the Harvard CMT catalog. Naming convention is mmddyy. Topography is from GTOPO30.

rupture plane striking 325° and dipping 55°NE (Figure 2). The top of the plane is at 20 km depth centered below 12.8°N, 89.0°W. Our model differs from the rupture plane given by *Bommer et al.* [2002] only in the strike. Although Bommer et al.'s modeled strike of 300° agrees more closely with the Harvard CMT focal mechanism nodal plane and parallels the strike of the trench in this region, our model derived strike is not geologically unreasonable, and is closely aligned with the fabric of outer-bend faults discussed by *Ranero et al.* [2005]. Using the coseismic offsets predicted by this model for our campaign site locations, we have corrected the estimated campaign site velocities (Figure 2 and Table 1). The modeled effects on campaign site velocities result in increasing the velocity magnitudes over a range from <0.1 mm yr^{-1} at the southern site ELBQ to ~1.8 mm yr^{-1} at the northernmost site, ELCO. Removal of the modeled offsets also results in a counterclockwise rotation of the velocity azimuths ranging from <1° at ELBQ to ~13° at ELCO. A similar elastic half-space dislocation model using the smaller rupture plane parameters of *Vallée et al.* [2003] with 3 m of slip differing again in strike (325° instead of their 297°) gives similar results with slightly greater predicted coseismic offsets at our campaign site locations. The smaller M_w 6.5 earthquake that occurred on February 13, 2001 did not produce significant coseismic offsets at SLOR or TEG1; therefore we did not insert any offsets for this event in our campaign site time-series.

5. Campaign Network Results

5.1. Backarc Sites

[9] Campaign sites in the backarc have small residual velocities (<5.5 mm yr^{-1}) relative to the stable Caribbean plate and within error appear to be part of the rigid Caribbean plate. Their small magnitudes compared to sites located in the forearc indicate that the forearc and backarc regions are moving independently from each other. The rigid Caribbean plate motion observed at these sites has

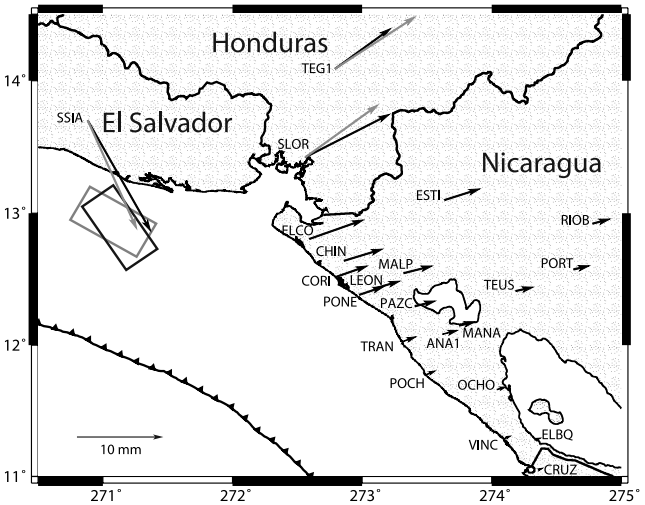

Figure 2. Coseismic offsets associated with the January 13, 2001 El Salvador earthquake at GPS sites in Nicaragua and surrounding region. Grey arrows are offsets calculated from continuous site time-series. Black arrows are predicted offsets from elastic half-space model. Black rectangle is the projection of rupture plane used in model. Grey rectangle is the projection of the rupture plane estimated by *Bommer et al.* [2002].

recently been examined by *DeMets et al.* [2007] and will not be discussed further here.

5.2. Forearc Sites

[10] Velocities for sites within the forearc are given in Table 1 and shown in Figure 1. The velocities for these sites are all directed toward the northwest and range from 7.6 ± 5.8 mm yr^{-1} at ELCO to 23.2 ± 5.7 mm yr^{-1} at CORI with a mean velocity of 15.1 mm yr^{-1}. The azimuths of the site velocities range from $\sim$276° to $\sim$331°, with a general trend for coastal and northern site velocities to point more westerly (Figure 1). The counterclockwise rotation of the site directions from the southeastern to the northwestern parts of the forearc generally follows the change in the trend of the trench.

6. Discussion

[11] GPS site velocities in the forearc region of Nicaragua are highly consistent in both direction and magnitude (Figure 1 and Table 1). The mean velocity for campaign sites in the forearc region is 15.1 mm yr^{-1} toward the northwest, which agrees remarkably well with the predicted 14 ± 2 mm yr^{-1} arc-parallel forearc sliver motion of *DeMets* [2001]. Campaign site velocities in the backarc region are much lower—essentially zero within error—indicating that they are moving as part of the stable Caribbean plate [*DeMets et al.*, 2007]. The boundary between the forearc and the stable Caribbean plate may be distinct, gradual, or broken into blocks as suggested by *LaFemina et al.* [2002]. Our current campaign network lacks the spatial density needed to distinguish among these models. Improved station density of the network is needed with the establishment of additional sites located in the Nicaraguan Depression to address this issue. The velocity determined for the continuous site MANA, which is located near the axis of the volcanic arc, is approximately half that of the nearby site ANA1, which is located to the southwest on the top of the Mateares fault scarp, suggesting that velocities fall off rapidly near the arc. The velocity of MALP, located near the arc axis, is also less than half that of the northern forearc sites supporting this hypothesis. Six additional sites were installed within the depression in February 2006 to further constrain the nature of the transition zone.

[12] In order to test whether the apparent motion of the forearc sliver is significant with respect to Caribbean plate motion, we compared a two plate model with a single plate model. In the two plate model, the twelve forearc sites listed in Table 1 were used to derive a weighted least squares best-fitting angular velocity vector for a forearc microplate. The stable Caribbean plate angular velocity was estimated using GPS velocities from the eastern Caribbean (AVES, BARB, CRO1, & ROJO), San Andres Island (SANA), and eastern Nicaragua (PORT, PUEC,RIOB, & TEUS). The single plate model estimated the best-fitting Euler pole for all of the GPS velocities listed above, including those in the forearc. An F-test comparing the separate forearc microplate model with the single Caribbean plate model indicates that the data are better fit by the two plate model at greater than the 99.9% confidence level [*Stein and Gordon*, 1984]. Our best-fitting Euler pole for Nicaraguan forearc sliver microplate (NI) motion relative to the Caribbean plate (CA) is located at N8.9°, W88.4° with a counterclockwise rotation rate of 1.957°/Ma.

[13] Residual velocities between observed forearc motion and that predicted by our best fitting Euler pole for forearc block motion appear to be randomly distributed. ELCO and CORI have the largest residuals and may indicate deformation across an unmapped structure in this region. Another possibility is that ELCO is near the sliver boundary (note its proximity to the arc) and is therefore showing reduced sliver motion. The residuals at ELBQ and VINC in the south show the slower motion of these sites compared with the rest of the forearc sites. The rms of the misfit for forearc sites is 4.9 ± 2.6 mm yr^{-1}. If the residuals of ELCO and CORI are excluded, the rms of the misfit drops to 3.5 ± 1.4 mm yr^{-1}. This value is substantially greater than that observed for larger plates with much more robust geodetic constraints [e.g., *Sella et al.*, 2002; *Calais et al.*, 2006], and leaves open the possibility of internal deformation in the microplate. The sources of this internal deformation might include elastic locking of forearc boundary faults and inter-forearc faults related to possible bookshelf faulting, or postseismic viscoelastic effects that vary across the network. The northwestern and southeastern boundaries of this forearc sliver have not yet been geodetically resolved. Some constraint on the southeastern boundary is provided by *Norabuena et al.* [2004] who observed an average of only 8 ± 3 mm yr^{-1} of trench-parallel motion in the Nicoya forearc, implying that the sliver boundary is near this region. Recent work by *Corti et al.* [2005] describes a right-lateral strike-slip fault system along the arc in El Salvador, indicating that sliver motion continues to the north beyond the Gulf of Fonseca. Future analysis of the velocity field of the forearc region in El Salvador as well as a combined study of the Nicaraguan and Costa Rican region is needed to investigate the boundaries of the sliver.

[14] Current motion of the forearc sliver relative to the stable Caribbean plate, assuming a boundary striking N50°W, yields predominantly boundary parallel motion of $\sim$14 mm yr^{-1}, with a very small component of arc-normal shortening in the southeastern region and with boundary-normal extension averaging $\sim$5 mm yr^{-1} in the region northwest of PAZC.

[15] The most surprising result of our campaign observations is the lack of a northeasterly-directed, arc-normal component of motion in the Nicaraguan forearc. This component of motion would be expected if mechanical coupling on the plate interface along this portion of the trench were strong [*Bevis and Martel*, 2001]. Since strong coupling is generally thought to be a prerequisite for strain partitioning and development of a forearc sliver [*Jarrard*, 1986], the lack of such a component in Nicaragua is somewhat perplexing. We are currently developing models for this section of the Middle America Trench to address this apparent lack of arc-normal strain accumulation, to identify the driving mechanism(s) for forearc motion, and to investigate coupling along the plate interface. One possible explanation for the missing arc-normal signal is that postseismic effects of the 1992 slow Nicaragua earthquake are masking the "normal" interseismic arc-normal component of strain accumulation. Another possibility is that this section of the trench is weakly coupled and arc-parallel forearc motion is being "pushed" from the SE by the

strongly coupled Nicoya Peninsula region in Costa Rica. Seismicity along this section of the trench, including the recent large events in Oct. 2004 and July 2005, however, contradicts this weakly-coupled hypothesis. It is interesting to note that GPS velocities along the Nicoya coast show large components of arc-normal strain, whereas the CRUZ site, located closer to the volcanic arc at a similar distance from the trench as those in our Nicaraguan forearc network shows almost pure arc-parallel motion (Figure 1) [*Lundgren et al.*, 1999; *Norabuena et al.*, 2004]. This suggests that the kinematic signature of strong coupling may lie offshore from the Nicaraguan portion of the Middle America Trench.

[16] **Acknowledgments.** This work was supported in part by NSF-EAR grants 0085432 and 0538135 and by NASA-UCR grant NCC5-518. We thank Wilfried Strauch and the personnel of INETER for their assistance with the field work. We thank Pedro Perez, Andy Eby, Curtis Nunn, and Wallis Hutton for their assistance in acquiring campaign observation data. Reviews by Chuck DeMets and an anonymous reviewer greatly improved the manuscript.

References

Bevis, M., and S. J. Martel (2001), Oblique plate convergence and interseismic strain accumulation, *Geochem. Geophys. Geosyst.*, *2*(8), doi:10.1029/2000GC000125.

Bommer, J. J., et al. (2002), The El Salvador earthquakes of January and February 2001: Context, characteristics and implications for seismic risk, *Soil Dyn. Earthquake Eng.*, *22*, 389–418.

Calais, E., J. Y. Han, C. DeMets, and J. M. Nocquet (2006), Deformation of the North American plate interior from a decade of continuous GPS measurements, *J. Geophys. Res.*, *111*, B06402, doi:10.1029/2005JB004253.

Corti, G., E. Carminati, F. Mazzarini, and M. O. Garcia (2005), Active strike-slip faulting in El Salvador, Central America, *Geology*, *33*, 989–992.

DeMets, C. (2001), A new estimate for present-day Cocos-Caribbean plate motion: Implications for slip along the Central American volcanic arc, *Geophys. Res. Lett.*, *28*, 4043–4046.

DeMets, C., G. S. Mattioli, P. E. Jansma, R. Rogers, C. Tenorios, and H. L. Turner (2007), Present motion and deformation of the Caribbean plate: Constraints from new GPS geodetic measurements from Honduras and Nicaragua, in *Geologic and Tectonic Development of the Caribbean Plate Boundary in Northern Central America*, edited by P. Mann, *Spec. Pap. Geol. Soc. Am.*, in press.

Harlow, D. H., and R. A. White (1985), Shallow earthquakes along the volcanic chain in Central America: Evidence for oblique subduction, *Earthquake Notes*, *55*, 28.

Jansma, P. E., and G. S. Mattioli (2005), GPS results from Puerto Rico and the Virgin Islands: Constraints on tectonic setting and rates of active faulting, in *Active Tectonics and Seismic Hazards of Puerto Rico, the Virgin Islands, and Offshore Areas*, edited by P. Mann, *Spec. Pap. Geol. Soc. Am.*, *385*, 13–30.

Jansma, P. E., G. S. Mattioli, A. Lopez, C. DeMets, T. H. Dixon, P. Mann, and E. Calais (2000), Neotectonics of Puerto Rico and the Virgin Islands, northeastern Caribbean, from GPS geodesy, *Tectonics*, *19*, 1021–1037.

Jarrard, R. D. (1986), Terrane motion by strike-slip faulting of forearc slivers, *Geology*, *14*, 780–783.

LaFemina, P. C., T. H. Dixon, and W. Strauch (2002), Bookshelf faulting in Nicaragua, *Geology*, *30*, 751–754.

Lundgren, P., M. Protti, A. Donnellan, M. Heflin, E. Hernandez, and D. Jefferson (1999), Seismic cycle and plate margin deformation in Costa Rica: GPS observations from 1994 to 1997, *J. Geophys. Res.*, *104*(B12), 28,915–28,926.

Mao, A., C. G. A. Harrison, and T. H. Dixon (1999), Noise in GPS coordinate time series, *J. Geophys. Res.*, *104*(B2), 2797–2816.

Marquez-Azua, B., and C. DeMets (2003), Crustal velocity field of Mexico from continuous GPS measurements, 1993 to June 2001: Implications for the neotectonics of Mexico, *J. Geophys. Res.*, *108*(B9), 2450, doi:10.1029/2002JB002241.

McCaffrey, R. (2002), Crustal block rotations and plate coupling, in *Plate Boundary Zones*, *Geodyn. Ser.*, vol. 30, edited by S. Stein and J. T. Freymueller, pp. 101–122, AGU, Washington, D. C.

Norabuena, E., et al. (2004), Geodetic and seismic constraints on some seismogenic zone processes in Costa Rica, *J. Geophys. Res.*, *109*, B11403, doi:10.1029/2003JB002931.

Ranero, C. R., A. Villasenor, J. Phipps Morgan, and W. Weinrebe (2005), Relationship between bend-faulting at trenches and intermediate-depth seismicity, *Geochem. Geophys. Geosyst.*, *6*, Q12002, doi:10.1029/2005GC000997.

Sella, G. F., T. H. Dixon, and A. Mao (2002), REVEL: A model for recent plate velocities from space geodesy, *J. Geophys. Res.*, *107*(B4), 2081, doi:10.1029/2000JB000033.

Stein, S., and R. G. Gordon (1984), Statistical tests of additional plate boundaries from plate motion inversions, *Earth Planet. Sci. Lett.*, *69*, 401–412.

Vallée, M., M. Bouchon, and S. Y. Schwartz (2003), The 13 January 2001 El Salvador earthquake: A multidata analysis, *J. Geophys. Res.*, *108*(B4), 2203, doi:10.1029/2002JB001922.

White, R. A. (1991) Tectonic implications of upper-crustal seismicity in Central America, in *Neotectonics of North America: Geological Society of America, Decade Map*, vol. 1, edited by D. B. Slemmons et al., pp. 323–338, Geol. Soc. of Am., Boulder, Colo.

T. Dixon, Rosenstiel School of Marine and Atmospheric Science, MGG, University of Miami, 4600 Rickenbacker Causeway, Miami, FL 33149, USA. (tdixon@rsmas.miami.edu)

P. LaFemina, Department of Geosciences, 503 Deike Building, Pennsylvania State University, University Park, PA 16802, USA. (plafemina@geosc.psu.edu)

P. E. Jansma, G. S. Mattioli, and H. L. Turner III, Department of Geosciences, 113 Ozark Hall, University of Arkansas, Fayetteville, AR 272701, USA. (pjansma@ uark.edu; mattioli@uark.edu)

A. Saballos, Dirección General De Geofísica, Instituto Nicaragüense de Estudios Territoriales, Frente a Policlínica Oriental. Apdo. Postal 2110, Managua, Nicaragua. (armando.saballos@gf.ineter.gob.ni)